

# Effect of low tailwater during drought on scour conditions downstream of an ogee spillway

Seung Ho Hong, Su Jin Kim, Terry Sturm & Thorsten Stoesser

*School of Civil and Environmental Eng.; Georgia Institute of Technology; Atlanta, Georgia USA*

Juan A González-Castro

*South Florida Water Management District; 3301 Gun Club Road; West Palm Beach, Florida 33406*

**ABSTRACT:** Low tailwater stages downstream of the stilling basin of an ogee spillway as a result of drought conditions can result in swept-out hydraulic jumps that enhance scour potential downstream of the structure. A hydraulic model study was conducted to assess the impact of low tailwater on energy dissipation provided by the stilling basin and the stability of the revetment lining in the downstream stilling pool. Detailed velocity and turbulence profiles were measured in the stilling pool for both submerged and swept-out hydraulic jumps. The results suggest that the primary scouring mechanism may be the impact of a submerged jet on the bed.

*Keywords: Drought, Hydraulic jump, Ogee spillway, Scour, Tailwater, Turbulence*

## 1 INTRODUCTION

### 1.1 Background and Purpose

Drought conditions such as those experienced in South Florida during 2007 and 2008 can induce extremely low tailwater stages downstream of Structure 65E, a low-head, gated ogee spillway located on the Kissimmee River which discharges into Lake Okeechobee (Turner and Pickering 1979, Personal Communication, South Florida Water Mgmt. District). During large floods, such low tailwater stages in the lake can lead to hydraulic jump properties that may enhance the scour potential immediately downstream of the structure and threaten its stability.

The purpose of the structure is to pass the design flood ( $680\text{m}^3/\text{s}$ ) without exceeding the upstream flood design stage. In addition, the structure limits the downstream design flood stages and channel velocities to non-damaging levels and passes low flows to maintain downstream stages and irrigation demands.

A hydraulic model study was conducted to further investigate the hydrodynamics of the flow downstream of the structure during conditions of low tailwater. Over a range of tailwater elevations from drought conditions to normal operation, the hydraulic jump either swept out of the stilling basin or was submerged by the tailwater. Sweeping

out of the jump under extremely low tailwater conditions resulted in erosion of the downstream riprap protection and complex flow patterns in the downstream stilling pool. Based on detailed velocity profiles and turbulence properties measured in the stilling pool and field observations of scour, it is suggested that the bed shear stress resulting from near-bed velocity gradients is not the primary mechanism of scour development, but rather it is a result of unsteadiness of the splatting event of large-scale flow structures transporting the high momentum of the near surface jet towards the bed in the area of scour.

## 2 EXPERIMENTAL STUDY

### 2.1 Modeling Similarity

The experimental setup is a fixed-bed, sectional model of the spillway and stilling basin which was constructed at a 1:30 undistorted geometric scale (length ratio,  $L_r = 1/30$ ) using Froude number similarity (see Figure 1.). At the chosen scale, the model Reynolds number based on spillway head is of the order of  $10^5$ , which ensures a fully turbulent flow regime as in the prototype (ASCE 2000). The model Weber number is estimated to be of the order of  $10^3$  which indicates that surface tension effects are negligible. The spillway crest and the

floor of the stilling basin are constructed of acrylic which minimizes roughness effects on the spillway flow even though they are already small because of the relatively small crest height.



(a) Ogee spillway and stilling basin



(b) Tailrace

Figure 1. Spillway model with vertical gates, piers, stilling basin and tailrace

The tailrace downstream of the spillway consists of a stilling pool with rock riprap revetment on the slope leading to the bottom of the stilling pool. The riprap in the model was modeled as a mobile bed and sized according to roughness similarity and Shields' criterion. To reproduce the riprap roughness in fully-rough turbulent flow, the relative roughness ratio of grain size to depth must be the same in model and prototype; that is,  $d_r/Y_r=1.0$  in which  $d_r$  is the grain size ratio and  $Y_r$  is the depth ratio. For a Froude number model, the depth ratio is equal to the length scale ratio  $L_r$ , so that the riprap is sized according to  $d_r=L_r$ . This satisfies Shields parameter similarity for initiation of motion if the specific gravity of the riprap is the same in model and prototype, the model is undistorted, and the particle Reynolds number is large enough which requires the model sediment size to be greater than about 1.5mm (coarse sand). This latter criterion is satisfied in the present model

study because the model riprap size becomes 15mm corresponding to the prototype size of 46cm.

The horizontal extent of the model is from 46m upstream of the spillway crest to a point 210m downstream of the spillway crest. This provides modeling of the region of an existing scour hole that has formed at the bottom of the riprap ramp. In this phase of the study only the riprap revetment was modeled as a mobile bed.

## 2.2 Experimental Measurements

Gate opening height ( $G_o$ ), headwater elevation ( $HW$  El.), tailwater elevation ( $TW$  El.), and discharge ( $Q$ ) were measured for seven test conditions as given in Table 1. The elevation of the crest of the spillway is 2.96m and the elevation of the floor of the stilling basin is  $-0.49$ m.

Table 1. Experimental Conditions ( $G_o$  = gate opening,  $HW$  El. = headwater elevation,  $TW$  El. = tailwater elevation,  $Q$  = discharge, subm. weir = submerged weir flow)

Flow Type	Hydr. Jump	$G_o$ (m)	$HW$ El.(m)	$TW$ El.(m)	$Q$ ( $m^3/s$ )
1-free orifice	swept out	2.07	6.71	0.01	509
2-free orifice	swept out	2.07	6.71	1.04	509
3-free orifice	swept out	2.07	6.71	2.31	510
4-free orifice	stable	2.16	6.71	3.43	533
5-free orifice	submerged	2.54	6.80	4.66	641
6-subm. weir	submerged	open	6.71	5.82	634
7-free weir	swept out	open	7.38	2.21	933

The gate openings were established by lowering the gates until they made a snug fit with an acrylic block that had been precision machined to the correct height relative to the spillway crest. The acrylic block was then carefully removed from under the gate without changing its position. The gates were held in place by friction between rubber gate gaskets and the gate slots. Then the flow rate was gradually increased with the tailgate raised (without submerging the spillway) until the target headwater was achieved. When the headwater had stabilized, the tailgate was adjusted to produce a tailwater elevation near the target value using a point gauge. Subsequently, the tailwater was measured more precisely with a capacitance wave gauge so that downstream waves could be averaged out to determine the mean tailwater elevation. The flow rate was measured with an electromagnetic flow meter, and the headwater was measured with a piezometer having an internal needle that could be adjusted to just touch the meniscus from below. Headwater elevations were measured 30.5m upstream of the spillway crest,

while tailwater elevations were taken at a distance of 91.5m downstream from the spillway crest.

Velocities and turbulence quantities were measured with a Son-Tek 16 MHz micro-ADV (acoustic Doppler velocimeter) with a measuring volume of  $0.09\text{cm}^3$  and sampling rates up to 50Hz. Previous investigators have used an ADV to measure the turbulent structure in hydraulic jumps of low Froude numbers (Liu et al. 2004) and turbulent flow characteristics of submerged hydraulic jumps on rough beds (Dey and Sarkar 2008). In this study, the measurements were made at 16 streamwise stations and approximately 10 vertical positions at each station to define the velocity and turbulence fields. The measurement locations were along two lines in the streamwise direction in the tailrace. Eight centerline measurement locations were aligned with the centerline gate pier while eight more locations were positioned at a distance of approximately 4.6m in the cross-stream direction from the structure centerline to coincide with the centerline of the gate bay. The streamwise spacing of the measurements was 9m just downstream of the riprap increasing to approximately 15m at the end of the tailrace.

Based on past experience with ADV measurements in a complex turbulence zone in the near-field of a model bridge pier (Lee and Sturm 2009; Ge et al. 2005), the required duration of the time record at each velocity measuring point was expected to be a minimum of 2min and perhaps as much as 10min. Dey and Sarkar (2008) reported sampling durations varying from 3 to 10min depending on the turbulence intensity for the case of a submerged hydraulic jump on a rough bed. Garcia et al. (2007) have suggested that optimum sampling time has to be decided on case-by-case basis depending on the turbulence characteristics. Accordingly, the optimum sampling duration was decided at the beginning of the test program by taking a continuous time record with a duration of three hours in the model tailrace. Then ensemble averages of velocities and turbulence quantities for various sampling durations were compared with the global 3-hr averages. Based on this analysis, a 5-min sampling duration was chosen.

For the purpose of determining the ADV sampling frequency that minimizes noise while assuring a representative turbulence signal, the guidelines developed by Garcia et al. (2005) were used to select a sampling frequency of 50Hz. Signal conditioning of the ADV measurements was completed as described by Lee and Sturm (2009) with despiking applied using the algorithm of Goring and Nikora (2002).

## 3 RESULTS

### 3.1 Description of flow types

Classifications of the flow type and the behavior of the hydraulic jump in the stilling basin for Test Conditions 1 to 7 are summarized in Table 1. The flow type for Test Conditions 1 to 5 can be classified as free orifice flow in which the tailwater has no influence on the measured headwater elevation. However for Test condition 5, vortices delivered air down the gate slots, and orifice flow could only be maintained by increasing the flow rate until the headwater increased to an elevation of 6.80m, which was slightly higher than the target value of 6.71m. At this point, a very small decrease in flow rate resulted in the free surface dropping below the gates into free weir flow. The gate opening was increased to 3.49m with a high tailwater elevation of 5.82m in Test Condition 6, which resulted in weir flow with no effect of the gates. In fact, the headwater was influenced by the tailwater so that the flow could be classified as a submerged weir flow. Finally, in Test Condition 7, the gates were fully open and the headwater elevation was set at the ogee design value of 7.38m (design head of 4.42m) by increasing the discharge with the tailwater set at approximately the same low value of Test Condition 3.

For the low tailwater of Test Conditions 1, 2, 3 and 7, the hydraulic jump swept out of the stilling basin and caused erosion of the downstream riprap in varying degrees of severity. Test Conditions 1 and 7 were the most severe with respect to stability of the riprap. Test Condition 1 was for the lowest tailwater elevation of 0.01m while Test Condition 7 was for a moderately low tailwater elevation of 2.21m but at the highest discharge. As shown in Figure 2 for Test Condition 1, the riprap was eroded off the floor of the downstream ramp and deposited in a broad low mound near the downstream toe of the ramp.

Test Condition 4 resulted in a stable hydraulic jump in the stilling basin. For Test Condition 5, the hydraulic jump was submerged on the face of the spillway without submerging the orifice flow under the gate as shown in Figure 3. Test condition 6 produced a very weak jump high on the face of the spillway, and it oscillated upstream and downstream reflecting the sensitive transition from free to submerged weir flow. In all three of these cases, the riprap was stable on the downstream slope.

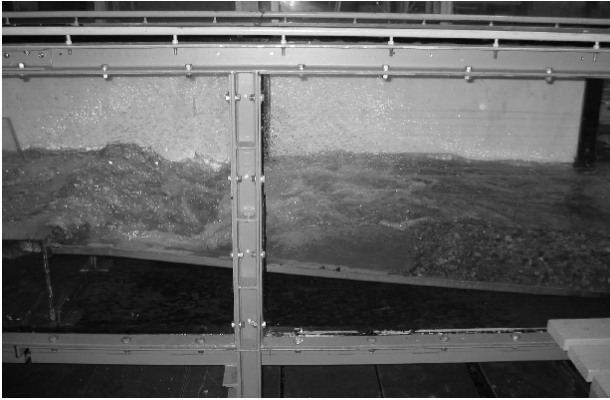


Figure 2. Hydraulic jump sweptout and riprap erosion for Test condition 1 with free orifice flow.

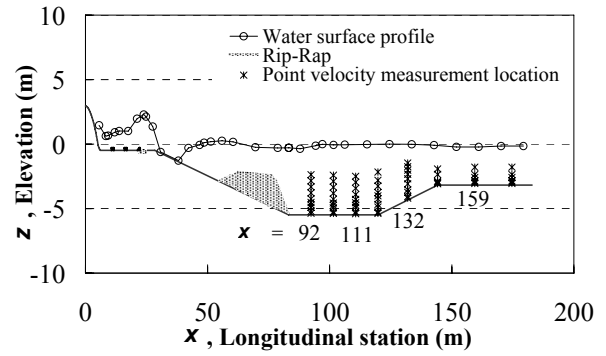


Figure 3. Submerged hydraulic jump for Test Condition 5 with free orifice flow and stable riprap.

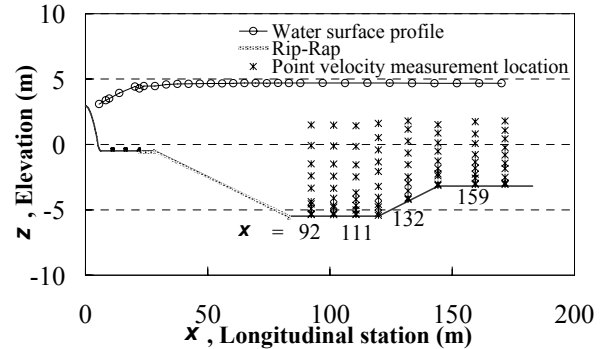
### 3.2 Experimental Data and Discussion

For the purposes of this paper, Test Conditions 1 and 5 as shown in Figures 2 and 3 are compared with respect to measured water surface profiles, velocity profiles and Reynolds stresses. The former condition corresponds to the extreme drought case of low tailwater while the latter is more representative of normal operating conditions for the spillway structure.

Water surface profiles for Test Conditions 1 and 5 are shown in Figure 4(a) and 4(b), respectively. In Test Condition 1 (Figure 4(a)), the low tailwater causes the jump to sweep out of the stilling basin with a high velocity jet that is flipped onto the downstream riprap-lined slope by the end sill of the stilling basin. At the impact point of the jet, the rock riprap is eroded off the downward slope of the stilling basin and deposited in a broad shallow mound at the foot of the slope. This results in a hydraulic jump on the face of the slope and a second high velocity flow over the riprap mound with an impact zone in the bottom of the stilling pool. A conceptual drawing of this flow pattern is shown in Figure 5.



(a) Test Condition 1: Free orifice flow at low tailwater with hydraulic jump swept out



(b) Test Condition 5: Free orifice flow with high tailwater and submerged hydraulic jump

Figure 4. Water surface profiles and locations of velocity profile measurements for Test Conditions 1 and 5.

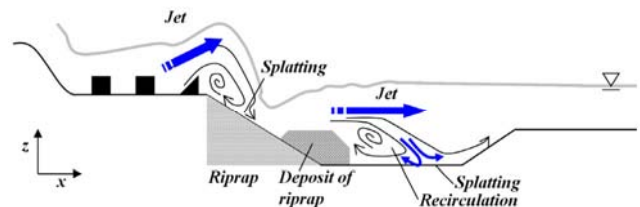


Figure 5. Conceptual flow pattern for Test condition 1.

The area of splating of the jet downstream of the redeposited riprap coincides with the location of an observed scour hole in the prototype which has a depth of approximately 3 m. This area was modeled as a fixed bed in the present study to measure the velocities and shear stresses in the scour zone before the occurrence of scour.

In contrast, Test Condition 5 at much higher tailwater has a water surface profile shown in Figure 4(b) that is nearly horizontal in the stilling pool area, and no riprap is eroded. Conceptually, flow velocities would be expected to decrease in the streamwise direction as the depth increases within the stilling pool, but much higher momentum fluid might be expected from the submerged jump as it exits the stilling basin in comparison to lower momentum fluid near the bed in the scour region. The conceptual flow pattern is shown in Figure 6.

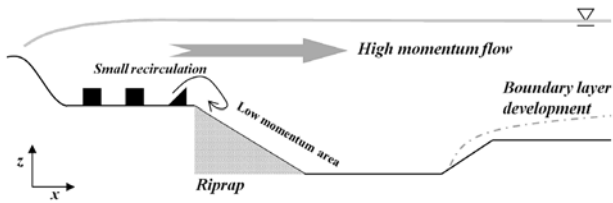


Figure 6. Conceptual flow pattern for Test condition 5.

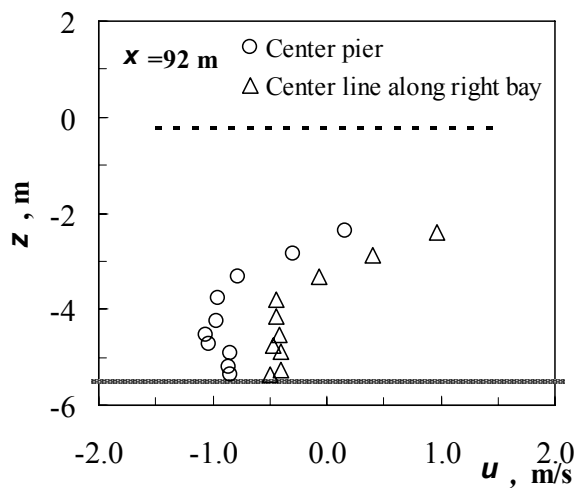
In order to further investigate the hypothesized flow patterns, velocity and turbulence profiles were measured at the locations shown in Figure 4 both at the structure centerline in alignment with the middle pier and along the centerline of the right-side spillway bay.

The flow over the riprap mound in Figure 4(a) is close to critical flow resulting in an accelerated jet which separates downstream of the deposited riprap. The velocity profiles in Figure 7(a) at  $x = 92\text{m}$  exhibit a reverse flow at the bed corresponding to a recirculation zone upstream of a submerged jet splatting at the impact point for Test Condition 1. Downstream of the impact point the

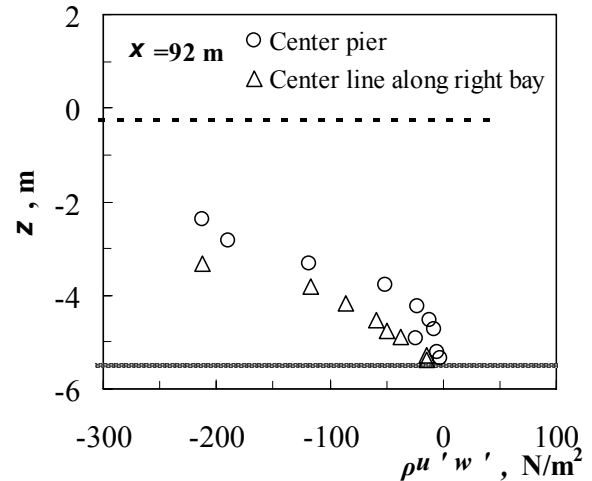
flow is accelerating near the bed as illustrated by the slight bulge and the positive velocities found there as shown in Figure 7(b). In the splatting event, high momentum fluid is swept towards the bed causing localized areas of high pressure that are expected to be responsible for erosion of the bed. The velocity profiles exhibit features similar to the recovering velocity profile behind a backward facing step or a sand dune (Stoesser et al. 2008).

Velocities in Figure 7 are weaker in the lee of the center pier in comparison with the centerline of the spillway gate bay. This difference persists both upstream and downstream of the impact of the submerged jet.

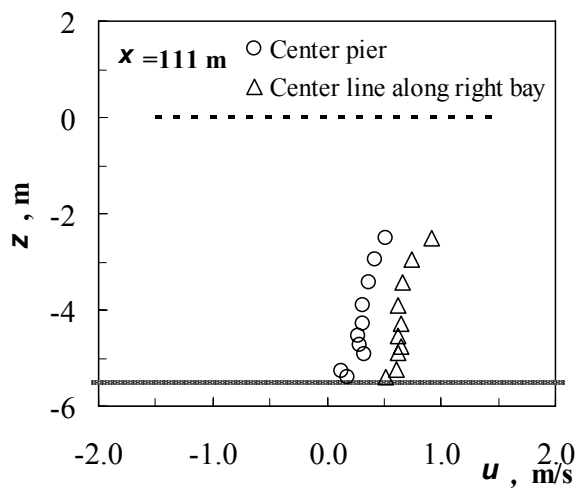
The conceptual model suggested in Figure 5 is further supported by the vertical distribution of the shear stress. Figure 8 presents the Reynolds shear stress at stations  $x = 92\text{m}$ , and  $x = 111\text{m}$ . A strong shear layer is formed due to the separated jet flow above the recirculation region. Towards the bed, the shear stress is decaying rather rapidly



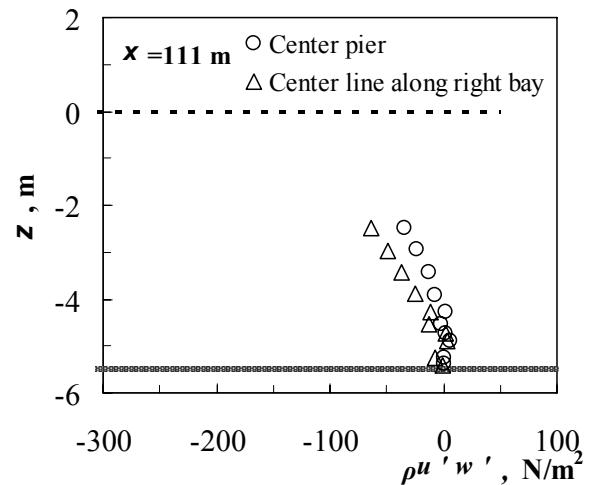
(a) Velocity profiles at  $x = 92\text{m}$



(a) Reynolds shear stress profiles at  $x = 92\text{m}$



(b) Velocity profiles at  $x = 111\text{m}$



(b) Reynolds shear stress profiles at  $x = 111\text{m}$

Figure 7. Velocity profiles, Test Condition 1

Figure 8. Reynolds shear stress profiles, Test Condition 1

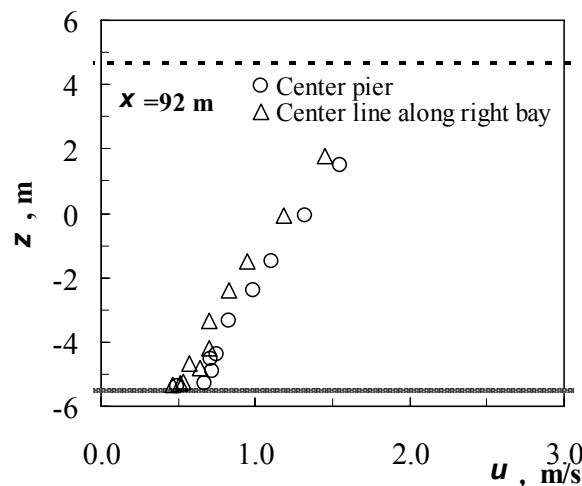
indicating very low momentum and turbulence in that region. This is strong evidence that the observed scour hole (in the field) downstream of the riprap is not caused by strong near-bed velocity gradients but by the splatting event.

As shown previously in Figure 6 for Test Condition 5, the flow is characterized by a submerged hydraulic jump in the stilling basin and high momentum flow above the downstream rip-rap lined slope. Velocity profiles indicate that there is no flow separation taking place; however, the flow immediately above the riprap is characterized by an area of low momentum fluid. Velocity and shear stress profiles are shown in Figure 9 at  $x=92\text{m}$  for Test Condition 5. These provide clear evidence for the statements made above; that is, the submerged jump creates an upper high momentum region in the stilling pool with a low momentum zone underlying it but without flow reversal in the bottom of the stilling pool. The velocity profile resembles more that of a mixing layer than a boundary layer. Relatively small turbulent shear stresses occur in the lower momentum region near the bed where the mixing layer is developing. The interface between high and low momentum flow is characterized by elevated values of shear stress around the area of  $z=0.0\text{m}$ , suggesting a shear layer between the two flow areas.

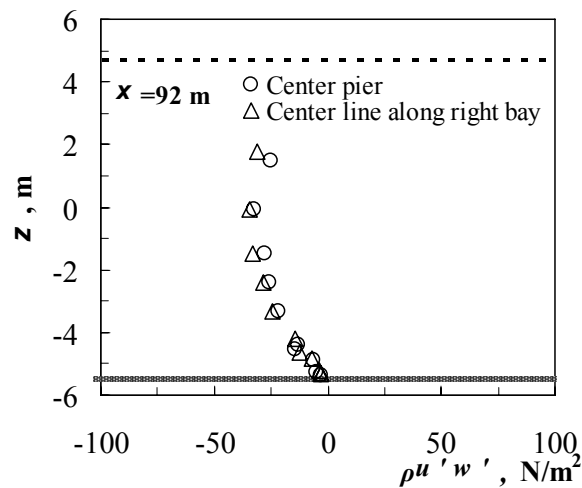
#### 4 CONCLUSIONS

Low tailwater during drought conditions has been shown to be a risk for scour downstream of a low-head ogee spillway operating under gate control. The hydraulic jump not only sweeps out of the stilling basin, but the flow exits as a jet thrown into the air by the end sill similar to the action of a flip bucket. The existing riprap downstream of the end sill is readily eroded by the impact of the jet and deposited near the base of the upstream slope of the stilling pool. The result is a stable hydraulic jump on the eroded downslope of the stilling pool with accelerated flow occurring over the deposited riprap mound. Downstream of the riprap mound, a submerged jet results in a splatting event at the point of jet impact with a recirculation zone upstream and a re-attached flow developing downstream of the point of impact. Turbulent shear stress profiles indicate very high shear in the upper portion of the flow, but a rapidly decaying shear stress in the lower portion. The dominant scour mechanism in the area of observed scour in the field appears to be splatting of large-scale flow structures transporting the high momentum of the near surface jet towards the bed. In contrast, a flow condition with a submerged hydraulic jump

on the stilling basin does not indicate flow reversal in the deeply submerged stilling pool, but it does display a shear layer resembling mixing layer flow with lower shear stresses near the bed. Based on this study it is suggested that for low tailwater conditions, the bed shear stress resulting from near-bed velocity gradients is not the primary mechanism of scour development but rather a result of large scale unsteadiness of the splatting event in the observed scour area. Additional studies are underway to further elucidate the scour mechanism in the spillway tailrace.



(a) Velocity profile at  $x = 92\text{m}$



(b) Reynolds shear stress profile at  $x = 92\text{m}$

Figure 9. Velocity and Reynolds shear stress profiles for Test Condition 5.

## ACKNOWLEDGMENTS

This study was conducted in accordance with the statement of work for contract 4500036521 between the South Florida Water Management District (SFWMD) and the Georgia Institute of Technology Water Resources Institute. Juan A. González-Castro acted as Project Manager and Terry Sturm and Thorsten Stoesser acted as Principal and Co-Principal Investigators, respectively. The last author gratefully acknowledges the support of Larry Deaton, Director of the Operations Control and Hydro Data Management Division of the SFWMD for his support of experimental work aimed at the understanding and reduction of scour at hydraulic structures.

## DISCLAIMER

The opinions presented here are those of the authors, they do not constitute the opinions of the SFWMD. Use of trade, product, or commercial names does not imply endorsement by the South Florida Water Management District.

## REFERENCES

- ASCE 2000. Hydraulic Modeling: Concepts and Practice. ASCE Manual No. 97, ASCE, Reston, VA.
- Dey, S. and Sarkar, A. 2008. Characteristics of turbulent flow in submerged jumps on rough beds. *J. Hydraul. Engrg.*, ASCE, 134(1), 49-59.
- Garcia, C.M., Cantero, M. I., Nino, Y., and Garcia, M. H. 2005. Turbulence measurements with acoustic Doppler velocimeters. *J. Hydraul. Engrg.*, ASCE, 131(12), 1062-1073.
- Garcia, C.M., Cantero, M. I., Nino, Y., and Garcia, M. H. 2007. Closure to Turbulence measurements with acoustic Doppler velocimeters. *J. Hydraul. Engrg.*, ASCE, 131(12), 1062-1073.
- Ge, L., Lee, S., Sotiropoulos, F., and Sturm, T. W. 2005. 3D unsteady RANS modeling of complex hydraulic engineering flows. Part II: Model validation and flow physics," *J. Hydraul. Engrg.*, ASCE, 131(9), 809-820.
- Goring, D. G., and Nikora, V. 2002. Despiking acoustic Doppler velocimeter data. *J. Hydraul. Engrg.*, 128(1), 117-126.
- Lee, Seung Oh and Sturm, T. W. 2009. Effect of sediment size scaling on physical modeling of bridge pier scour. *J. Hydraul. Engrg.*, 135(10), 793-802.
- Liu, M., Rajaratnam, N., and Zhu, D. 2004. Turbulent structure of hydraulic jumps of low Froude numbers. *J. Hydraul. Engrg.*, ASCE, 130(6), 511-520.
- Stoesser, T., Braun, C., Garcia-Villalba, M., Rodi W. 2008. Turbulence structures in flow over two dimensional dunes. ASCE, *J. Hydraul. Engrg.*, 134 (1), pp. 42-55.
- Turner, H. O. Jr., and Pickering, G. A. 1979. Kissimmee River Structures, Central and Southern Florida Flood Control Project. Tech. Rpt. HL-79-4, U. S. Army Engineer Waterways Experiment Station, Vicksburg, MS.